Applying an optical space-time coding method to enhance light scattering signals in microfluidic devices

Zhe Mei,[1,2] Tsung-Feng Wu,[3] Luca Pion-Tonachini,[2] Wen Qiao,[2]
Chao Zhao,[3] Zhiwen Liu,[1] and Yu-Hwa Lo[2,3]
[1]*School of Information and Electronics, Beijing Institute of Technology, Beijing 100081, China*
[2]*Department of Electrical and Computer Engineering, University of California San Diego, La Jolla, California 92093-0407, USA*
[3]*Materials Science and Engineering Program, University of California at San Diego, La Jolla, California 92093-0418, USA*

(Received 4 June 2011; accepted 23 July 2011; published online 16 August 2011)

An "optical space-time coding method" was applied to microfluidic devices to detect the forward and large angle light scattering signals for unlabelled bead and cell detection. Because of the enhanced sensitivity by this method, silicon pin photoreceivers can be used to detect both forward scattering (FS) and large angle (45–60°) scattering (LAS) signals, the latter of which has been traditionally detected by a photomultiplier tube. This method yields significant improvements in coefficients of variation (CV), producing CVs of 3.95% to 10.05% for FS and 7.97% to 26.12% for LAS with 15 μm, 10 μm, and 5 μm beads. These are among the best values ever demonstrated with microfluidic devices. The optical space-time coding method also enables us to measure the speed and position of each particle, producing valuable information for the design and assessment of microfluidic lab-on-a-chip devices such as flow cytometers and complete blood count devices. © *2011 American Institute of Physics*. [doi:10.1063/1.3624740]

Particle counting and differentiation based on optical detection in microfluidic devices has attracted significant attention because the technology promises cheaper, portable, and easy-to-operate devices for research, clinical, environmental, and industrial applications.[1–4] In a conventional design, the suspended particles in a microfluidic channel are directed in a stream to an interrogation area where optical scattering, fluorescence, and Raman signals as well as electrical signals such as impedance are detected to reveal the intrinsic properties of the sample. According to the detected signals, particle separation methods based on hydrodynamic, dielectrophoretic, optical, acoustic, or magnetic mechanisms may be applied to direct the particles to the designated downstream channels, a function called cell sorting to isolate subpopulations of cells from the biological sample.[5–7] For both sample analysis and sorting, detection of the intrinsic properties of each particle is the most critical step and is particularly important for single-cell analysis in contrast with detection of the average properties of an ensemble. Here, forward scattering (FS) and large angle scattering (LAS) or side-scattering (SS) signals are the most commonly used signals for bead and cell analysis since these signals reveal the size, shape, and granularity of each individual particle without the need for labeling which adds complexity, cost, and potentially bias to the subjects. However, side scattering signals are orders of magnitude weaker and usually detected by photomultiplier tubes (PMTs) which require high voltage (>1000 V) operation and are expensive and fragile, not suitable for point-of-care clinics.[8,9] Furthermore, most microfluidic devices produce weaker and more noisy side scattering signals than commercial systems, and the large coefficients of variation (CV) values of microfluidic devices have severely limited the applicability of the side scattering signals in devices such as flow cytometers and complete blood count (CBC) devices.[10]

In this paper, we present an optical space-time coding technique to detect both forward (5–10°) and large angle (45-60°) scattering signals using commodity Si PIN photoreceivers instead of sophisticated PMTs. Specially designed patterns were deposited on the microfluidic

channel area as a spatial mask to shape the illumination pattern upon the particle travelling through the detection area. The spatial mask turns the scattering signals from travelling particles into a temporal waveform, which gives the technique the name of "space-time" coding. By introducing a time based carrier to overlay the signal, one can filter out the elements in the spectrum outside the carrier band. This technique could also be viewed as an extension of the direct sequence spread spectrum technology widely used in communication systems.[11,12] The temporarily coded signal can be easily distinguished from the noise and the signal-to-noise ratio can be enhanced using numerous digital signal processing techniques including digital filters, matched filters, etc., enabling detection of the weak large angle scattering signals using an Si pin detector with good CV values. Furthermore, information about the travel speed and the position of the particle within the microfluidic channel can also be acquired via the waveform. Such information is important for flow cytometers, CBC devices, and microfluidic devices in general because it enables users to measure the quality of flow confinement. If applications require cell sorting such as in fluorescence-activated cell sorter (FACS), knowing travel speed of each individual particle can significantly improve the sample purity and sorting yield.[13]

Figure 1(a) shows the schematic of measurement setup. A 488 nm wavelength diode laser (40 mW, Spectra-physics) was used as the light source. The laser beam had a Gaussian intensity profile across the sensing area of 450 μm. Two silicon photoreceivers (PDA36A, Thorlabs) were placed over the microfluidic device to detect FS and LAS synchronously from particles passing the sensing area. The signals were collected by off-the-shelf software (Signal Express, National Instrument) and processed with MATLAB (Version 7.8.0.347, MathWorks) installed on a desktop computer.

The microfluidic device with a spatial mask was fabricated in polydimethylsiloxane (PDMS, Sylgard 184, Dow Corning) using standard soft lithography technique. The straight channel is 5 cm in length with a cross-section of 100 μm $\times$ 45 μm (width $\times$ height). Over the interrogation area where the scattering signal was detected, four transparent trapezoidal slits were formed as a spatial mask by patterning a thin Ti/Au metal film on the glass substrate. Each trapezoidal slit has its base lengths of 100 μm and 50 μm. Fours slits separated by 50 μm between each other were located 4.5 cm from the inlet. In this experiment, a mixture of polystyrene beads with diameters of 5, 10, and 15 μm (PPS-6K, Sphero) were injected into the microfluidic channel with the flow rate controlled by a syringe pump (NE-1000, New Era Pump Systems).

As shown in Figure 1(b), a scattering signal of a specific waveform is generated by the four transparent slits according to the position of the particle that passes through. Because of the trapezoid slit design, the ratio of pulse width P2 to P1 is between 2 and 0.5. The values 2 and 0.5 correspond to two opposite ends of the mask or the edges of the microfluidic channel,

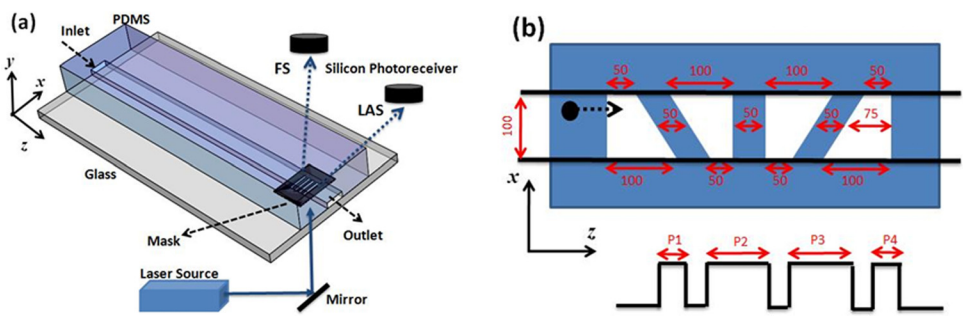

FIG. 1. (a) Test setup and design of the optical space-time coded microfluidic device. The samples enter the microfluidic channel from the inlet by a syringe pump. The laser beam illuminates the microfluidic channel through the mask with a pattern in (b). FS and LAS represent forward scattering and large angle scattering signals detected by 2 Si PIN photoreceivers with a 3×3 mm^2 photosensitive area. (b) The detailed design of the spatial mask. Four transparent trapezoidal slits are formed on the mask to encode the waveforms of particles depending on their travel positions. Below the mask pattern is the schematic of an ideal waveform showing 4 peaks with pulse width P1 to P4 corresponding to the bead's position along the x-direction.

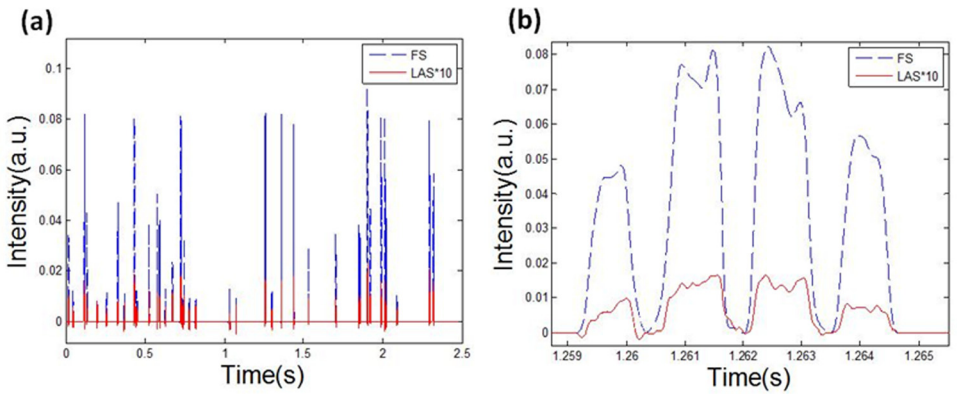

FIG. 2. (a) Forward (blue) and large angle side scattering (red) signals for a mixture of 5, 10, and 15 μm beads. (b) The close-up view of one event. The dash line depicts the forward scattering signal and the solid line depicts the large angle scattering. (a) and (b) are signals after a low pass filter with a cutoff frequency of 2500 Hz.

and the P2/P1 ratio of 1 corresponds to the center of the channel along the channel width. The velocity of each particle can also be obtained by dividing the pattern width (450 μm) by the duration of the waveform.

To reduce the complexity of device fabrication and operation without losing the purpose of proving the key concepts of optical space-time coding, no features for flow confinement were incorporated into our design. As a result, coincident events, meaning more than two particles simultaneously pass the interrogation area, occurred to our device more frequently than typical microfluidic devices with sheath flow. Those signals produced by coincident events were identified since they lacked the 4 distinctive peaks which are characteristics of signals from single events. Those coincident events were then excluded from the analysis.

Figures 2(a) and 2(b) are typical space-time coded FS and LAS signals produced by bead samples. The displayed signals have gone through a high pass digital filter (cutoff frequency: 250 Hz) to remove low frequency noise and any baseline drift. A standard peak-finding algorithm based on a predefined threshold was employed in MATLAB to register all detectable events. In our experiment, the gain of amplifier is 50 dB for LAS detection and 30 dB for FS detection since the LAS signals are much weaker than FS signals. To show both signals on the same chart, the LAS signals were also plotted at 10$\times$ of the measured amplitudes. Due to the Gaussian intensity profile of the laser beam, the two central peaks of the space-time coded signals have higher magnitudes than the two side peaks. The quality of the signals, particularly the more noisy LAS signals, can be enhanced using several digital signal processing algorithms enabled by their special waveforms. Such algorithms include matched filter, cross correlation between the stronger FS signal and the weaker LAS signal, etc. We have shown that, for practical purposes, even the simplest algorithm of taking the average of the magnitudes of 4 distinct peaks in the waveform can significantly improve the CV values of both FS and LAS signals. For the rest of the paper, we have adopted this simple algorithm for data analysis since this algorithm requires a minimum amount of computation and favors real time processing required by cell sorting.

Figure 3(a) shows the distribution plot of LAS intensity versus FS intensity from a sample consisting of a mixture of 5 μm, 10 μm, and 15 μm polystyrene beads. The scatter plot from a commercial flow cytometer (C6 flow cytometer, Acurri) is shown in Fig. 3(b) for comparison. It is clear that larger beads produce higher FS and LAS (or side scattering for the commercial system) intensities and three types of beads form three separate clusters that are easy to distinguish. For data from the commercial flow cytometer, there are also signals very close to the origin likely due to debris or impurities in the sample and system noise. Such data are not shown in our result because the signal processing has removed those points. To further demonstrate the performance improvements using the proposed method, we ran experiment using the same setup without the spatial mask and the result is shown in Figure 3(c). In sharp contrast to

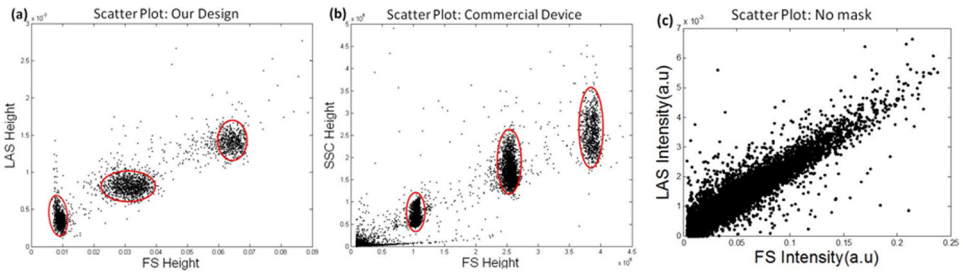

FIG. 3. Data plots for a mixture sample of 5 μm, 10 μm, and 15 μm beads. (a) FS-LAS scatter plot of our design (with the spatial mask). (b) FS-SSC scatter plot of a commercial flow cytometer. (c) FS-LAS scatter plot of a microfluidic device without the spatial mask. The flow rate is 25 μl/min.

Figure 3(a), without the spatial mask one cannot obtain 3 distinct groups in the distribution plot corresponding to 5 μm, 10 μm, and 15 μm beads. By employing the quadrant gate, CVs of each bead population from our device (with the spatial mask) and the commercial flow cytometer are summarized in Table I.

The FS CVs measured from our device are 10.05%, 9.53%, and 3.95% for 5 μm, 10 μm, and 15 μm beads, respectively. These values are about 3 times of the CVs from the commercial system. We suspect that the laser speckle noise and the interference effects caused by the spatial mask may contribute to the signal fluctuation of the FS signal shown in Fig. 2(b). Nonetheless, these are among the best values achieved with microfluidic devices.[14]

On the other hand, the CVs of large angle signals from our device are compared favorably with the CVs of side-scattering signals from the commercial device, and the improvements are quite significant for 10 and 15 μm beads. Keep in mind that the LAS signal was detected by a low cost Si photoreceiver bias at 5 V as opposed to a PMT biased at 1500 V and the CV values of the LAS signals set the new record for microfluidic devices. Hence, we believe the optical space-time coding method is not only compatible with the microfluidic platform but also particularly suitable for point-of-care applications where low cost, simple operation and quality of results are key concerns.

Besides reducing the noise and CV values for FS and LAS signals, the optical space-time coding method also offers the unique capabilities to measure the position and velocity of each particle in the microfluidic channel. The velocity information can be easily obtained from the spacing between the slits and the time difference between the peaks in the waveform. As we have 4 peaks produced by 4 slits in the spatial mask, the speed of travel can be obtained from multiple measurements to reduce errors. Based on the special design of the spatial mask (Fig. 1(b)), there exists a simple relation between the ratio of the pulse width of each peak and the position of the particle. Figure 4 shows two distribution plots: bead position versus FS intensity (Fig. 4(a)) and velocity versus FS intensity (Fig. 4(b)), for the mixture of 5 μm, 10 μm, and 15 μm beads at a flow rate of 25 μl/min. Around 3000 events were processed and included in the figure. The data in Fig. 4(a) suggest that, without flow focusing or sheath flow, 5 μm beads spread widely over the entire 100 μm width of the microfluidic channel whereas 10 μm and 15 μm beads were more concentrated to a narrow range of the channel. This is a clear demonstration of the effect of inertial focusing governed by the "particle Reynolds number."[15] The results also shed light on the feasibility and effectiveness of using fluid dynamics

TABLE I. Scatter intensity CVs.

	FS CV (our design)	FS CV (commercial device)	LAS CV (our design)	SSC CV (commercial device)
5 μm	10.05%	3.38%	26.12%	22.33%
10 μm	9.53%	2.78%	11.5%	16.85%
15 μm	3.95%	1.97%	7.97%	14.09%

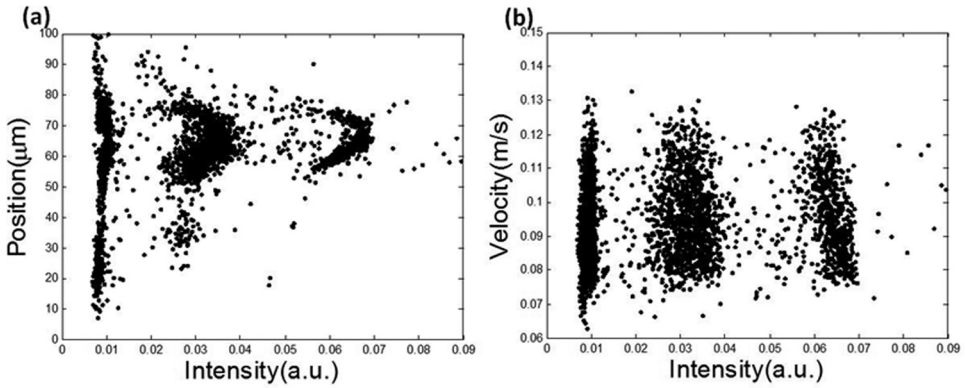

FIG. 4. Data plots for a mixture sample of 5 μm, 10 μm, and 15 μm beads. (a) Scattering plots of particle position along x-axis versus forward scattering intensity. (b) Particle velocity versus intensity. The flow rate is 25 μl/min. For both figure, from left to right, each group indicate 5 μm, 10 μm, and 15 μm beads, respectively.

properties to separate particles. On the other hand, data in Fig. 4(b) show that beads of all the three sizes had similar velocity distributions except a lower number of 10 μm and 15 μm beads that had lower speed because they were further away from the channel edge. More detailed analysis of particle distributions in microfluidic channels can be found in Ref. 16.

Finally, to study the applicability of our design to cells in addition to beads, preliminary experiment on lymphocyte was conducted and the result was compared with that of a commercial flow cytometer. As shown in Figure 5, both tests show wide distributions in the intensity of FS and LAS (side scattering) signals because of the intrinsic characteristics of lymphocyte. Again, the system noise near the origin of the plot was absent in our device because our signal processing algorithms for the space-time coded signal remove the background noise. Under similar operation time, our device produced 3000 events versus approximately 15 000 events from a commercial flow cytometer at a flow rate of 25 μl/min. The lower throughput was partly caused by the high probability of co-incident events due to the lack of a sheath flow. Nonetheless, the adequate sensitivity level of the forward and large angle scattering signals and the similar signal distribution to the commercial flow cytometers show the feasibility of our optical space-time coding technique for biological samples.

To summarize, we have demonstrated an optical space-time coding method that can be easily incorporated into microfluidic devices to aid the detection of forward and large angle scattering signals. Because of the enhanced signal quality by the new technique, one can detect large angle (45–60°) scattering signals using a silicon PIN photoreceiver without the usual PMT detector, resulting in significant cost saving and simplification in operation to favor point-

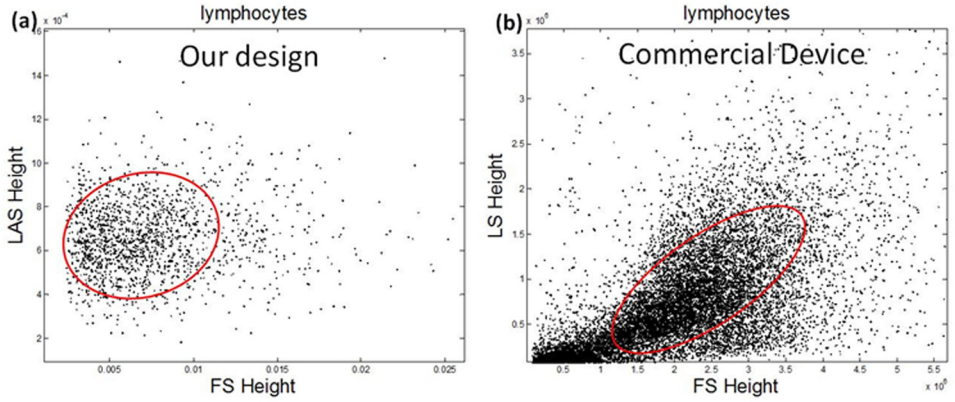

FIG. 5. Data plots of lymphocyte sample. (a) FS-LAS scatter plot of our design. The flow rate is 25 μl/min. (b) FS-SSC scatter plot of a commercial flow cytometer.

of-care applications. The optical space-time coding technique also enables us to set the performance records for large-angle scattering CVs among microfluidic devices. The feasibility of the technique has also been verified with lymphocyte samples, showing comparable signal pattern with commercial systems. Finally, we have demonstrated that the optical space-time coding technique also contains valuable information about the position and velocity of the particles in a microfluidic channel, shedding light on important properties of microfluidic devices such as inertial focusing and fluid dynamic sample separation.

The authors acknowledge the technical support of the staff of the UCSD Nano3 (Nanoscience, Nanoengineering, and Nanomedicine) Facility in Calit2. This work was supported by NIH grants R01HG004876, R21RR024453, and R43RR031424. One of the authors, Zhe Mei, was supported by China Scholarship Council and National Natural Science Foundation of China No. 61001063.

[1]S. Cho, J. Godin, C. Chen, W. Qiao, H. Lee, and Y. Lo, Biomicrofluidics **4**, 043001 (2010).
[2]P. Yager, T. Edwards, E. Fu, K. Helton, K. Nelson, M. Tam, and B. Weigl, Nature (London) **442**, 412 (2006).
[3]P. Rezai, A. Siddiqui, P. Selvaganapathy, and B. Gupta, Lab Chip **10**, 220 (2010).
[4]S. Neethirajan, I. Kobayashi, M. Nakajima, D. Wu, S. Nandagopal, and F. Lin, Lab Chip **11**, 1574 (2011).
[5]J. Godin, C. Chen, S. Cho, W. Qiao, F. Tsai, and Y. Lo. J. Biophotonics **1**, 355 (2008).
[6]A. Valeroa, T. Braschler, N. Demierre, and P. Renaud, Biomicrofluidics **4**, 022807 (2010).
[7]D. Ateya, J. Erickson, P. Howell, L. Hilliard, J. Golden, and F. Ligler, Anal. Bioanal. Chem. **39**, 1485 (2008).
[8]N. Pamme, R. Koyama, and A. Manz, Lab Chip **3**, 187 (2003).
[9]Z. Wang, J. El-Ali, M. Engelund, T. Gotsaed, I. R. Perch-Nielsen, K. B. Mogensen, D. Snakenborg, J. P. Kutter, and A. Wolff, Lab Chip **4**, 372 (2004).
[10]C. Song, T. Luong, T. Kong, N. Nguyen, and A. Asundi, Opt. Lett. **36**, 657 (2011).
[11]P. Kiesel, M. Bassler, M. Beck, and N. Johnson, Appl. Phys. Lett. **94**, 041107 (2009).
[12]R. Dixon, *Spread Spectrum Systems with Commercial Applications*, 3rd ed. (Wiley, New York, 1994).
[13]S. Cho, C. Chen, F. Tsai, J. Godin, and Y. Lo, Lab Chip **10**, 1567 (2010).
[14]J. Godin and Y. Lo, Biomed. Opt. Express **1**, 1472 (2010).
[15]D. Gossett, W. Weaver, A. Mach, S. Hur, H. Tse, W. Lee, H. Amini, and D. Carlo, Anal. Bioanal. Chem. **397**, 3249 (2010).
[16]T. Wu, Z. Mei, L. Tonachini, C. Zhao, W. Qiao, A. Arianpour, and Y. Lo, AIP Adv. **1**, 022155 (2011).